Int. J. Heat Mass Transfer. Vol. 33, No. 1, pp. 55–60, 1990
Printed in Great Britain

0017–9310/90 $3.00 + 0.00

Linear stability of convection in a rigid channel uniformly heated from below

P. G. DANIELS and C. F. ONG
Department of Mathematics, City University, Northampton Square, London EC1V 0HB, U.K.

(*Received* 19 *April* 1989)

Abstract—A two-dimensional Galerkin formulation of the three-dimensional Oberbeck–Boussinesq equations is used to determine the onset of convection in an infinite rigid horizontal channel uniformly heated from below. Earlier results (Chana and Daniels, *J. Fluid Mech.* **199**, 257–279 (1989)) are extended to higher levels of truncation and to include modes of convection not previously examined.

1. INTRODUCTION

THERMAL convection is an important mechanism of heat and mass transfer in many different areas and there are an increasing number of technological applications where the flow is partly or completely confined. Theoretical work on the onset of convection in boxes heated from below includes that by Davis [1] and Catton [2] and experimental work has been carried out by Buhler *et al.* [3] and Luijkx *et al.* [4]. An idealized model of convective instability in an infinite rectangular channel uniformly heated from below was considered by Davies-Jones [5] who used the assumption of stress-free horizontal boundaries to simplify the mathematical analysis. More recently, solutions have been found for rigid boundaries [6] using a two-dimensional Galerkin formulation of the Oberbeck–Boussinesq equations, which, for steady linearized motion with respect to Cartesian coordinates x, y, z can be written as

$$\frac{\partial u}{\partial x}+\frac{\partial v}{\partial y}+\frac{\partial w}{\partial z}=0, \quad \nabla^2 u=\frac{\partial p}{\partial x}, \quad \nabla^2 v=\frac{\partial p}{\partial y}$$

$$\nabla^2 w+R\theta=\frac{\partial p}{\partial z}, \quad \nabla^2\theta+w=0 \tag{1}$$

where (u, v, w), θ and p are respectively the non-dimensional velocity components, temperature and pressure measured relative to the basic state of constant stratification and no motion. The non-dimensional coordinates are located with the x-axis along the centre of the horizontal channel and the z-axis vertically upwards. The Rayleigh number is defined as

$$R=\alpha g\Delta\theta^* d^3/\kappa\nu \tag{2}$$

where α is the coefficient of thermal expansion, g the acceleration due to gravity, $\Delta\theta^*$ the temperature difference maintained between the lower and upper surfaces of the channel, d the height of the channel and κ and ν the thermal diffusivity and kinematic viscosity, respectively. The second parameter involved in the determination of the occurrence of weakly nonlinear stationary states is the semi-aspect ratio a of the cross-section of the channel, $|y| \leqslant a$, $|z| \leqslant \frac{1}{2}$. The walls of the channel are assumed to be rigid and perfectly conducting so that

$$u=v=w=\theta=0 \tag{3}$$

on $y=\pm a$ and $z=\pm\frac{1}{2}$.

Solutions of equations (1) and (3) are sought in the form

$$(\theta, u, v, w, p)=\mathrm{e}^{\mathrm{i}qx}(\Theta, iU, V, W, P)(y, z) \tag{4}$$

where q is a wave number for variations along the channel. Substitution into equation (1) and elimination of U and P yields the reduced system

$$\left(\frac{\partial^2}{\partial y^2}+\frac{\partial^2}{\partial z^2}-q^2\right)\left(\left(\frac{\partial^2}{\partial y^2}-q^2\right)V+\frac{\partial^2 W}{\partial y\,\partial z}\right)=0 \tag{5}$$

$$\left(\frac{\partial^2}{\partial y^2}+\frac{\partial^2}{\partial z^2}-q^2\right)\left(\left(\frac{\partial^2}{\partial z^2}-q^2\right)W+\frac{\partial^2 V}{\partial y\,\partial z}\right)-Rq^2\Theta=0 \tag{6}$$

$$\left(\frac{\partial^2}{\partial y^2}+\frac{\partial^2}{\partial z^2}-q^2\right)\Theta+W=0 \tag{7}$$

for V, W and Θ, to be solved subject to

$$\left.\begin{aligned} V=\frac{\partial V}{\partial y}=W=\Theta=0 \quad & \text{on } y=\pm a \\ V=W=\frac{\partial W}{\partial z}=\Theta=0 \quad & \text{on } z=\pm\tfrac{1}{2}. \end{aligned}\right\} \tag{8}$$

The total flux down the channel is zero for non-zero wave numbers q, with

$$U=\frac{1}{q}\left(\frac{\partial V}{\partial y}+\frac{\partial W}{\partial z}\right). \tag{9}$$

NOMENCLATURE

a semi-aspect ratio of channel
a_k, b_k, c_k Galerkin coefficients
d height of channel
g acceleration due to gravity
N Galerkin truncation level
p non-dimensional pressure
P pressure function
q wave number
R Rayleigh number
u, v, w non-dimensional velocity components
U, V, W velocity functions
x, y, z non-dimensional coordinates.

Greek symbols
α coefficient of thermal expansion
θ non-dimensional temperature
$\Delta\theta^*$ vertical temperature difference
Θ temperature function
κ thermal diffusivity
ν kinematic viscosity.

2. GALERKIN FORMULATION

The system of equations and boundary conditions (5)–(8) can be solved by a Galerkin method in which

$$\Theta = \sum_{k=1}^{N} a_k \Theta_k(y,z), \quad W = \sum_{k=1}^{N} b_k W_k(y,z),$$
$$V = \sum_{k=1}^{N} c_k V_k(y,z) \tag{10}$$

for a specified truncation level N. Solutions can be classified according to y, z symmetries shown in Table 1; in ref. [6] only the leading even–even (EE) mode was considered, corresponding to trial functions

$$\Theta_k = \cos(2m-1)\frac{\pi y}{2a}\cos(2n-1)\pi z$$
$$W_k = C_n(z)\cos(2m-1)\frac{\pi y}{2a}$$
$$V_k = S_m\left(\frac{y}{2a}\right)\sin 2n\pi z. \tag{11}$$

Here C_n and S_m are the beam functions discussed by Harris and Reid [7]. Values of m and n are assigned to values of k according to the pattern shown in Table 2; the maximum truncation level considered in ref. [6] was $N = 10$. Here results are extended to much higher truncation levels ($N = 25$), incorporating all individual y and z modes up to $m = 5$ and $n = 5$. In addition, higher modes of convection are determined, including the second EE mode and the first two odd–even (OE) modes, the main purpose being to establish that the EE mode determined in ref. [6] is the first to appear as the Rayleigh number is increased. The remaining even–odd (EO) and odd–odd (OO) modes, which are expected to be of most significance in relatively thin channels, are not examined. Results for the leading mode in the case of insulating sidewalls are described by Luijkx and Platten [8].

For the OE mode the trial functions are taken to be

$$\Theta_k = \sin\frac{m\pi y}{a}\cos(2n-1)\pi z$$
$$W_k = C_n(z)\sin\frac{m\pi y}{a}$$
$$V_k = C_m\left(\frac{y}{2a}\right)\sin 2n\pi z \tag{12}$$

consistent with boundary conditions (8). The series (10) are substituted into equations (5)–(7) which are then multiplied by $V_{\bar{k}}$, $W_{\bar{k}}$ and $\Theta_{\bar{k}}$ ($\bar{k} = 1, \ldots, N$), respectively, and integrated over the cross-section of the channel to obtain a set of $3N$ linear algebraic equations for the coefficients a_k, b_k and c_k, making use of orthogonality properties where appropriate (see ref. [6]). The double integrals are converted into multiplicative combinations of single integrals which are then evaluated using Simpson's rule, typically with 200 intervals, ensuring no measurable loss of accuracy from this source in comparison with that from truncation effects. The zeros of the determinant of the coefficient matrix are found by using Newton's method to adjust the value of R at a given value of q.

Table 1. y, z symmetries of eigenmodes: E, even; O, odd

Mode	EE		OE		EO		OO	
	y	z	y	z	y	z	y	z
Θ, W	E	E	O	E	E	O	O	O
V	O	O	E	O	O	E	E	E

Table 2. Ordering of trial functions

	k															
	1	2	3	4	5	6	7	8	9	10	11	12	13	14	15	16
m	1	1	2	2	1	2	3	3	3	1	2	3	4	4	4	4
n	1	2	1	2	3	3	1	2	3	4	4	4	1	2	3	4

Table 3. Convergence of the Galerkin scheme for $a = 1/2$

N	q_c	R_c	a_1	b_1	a_2	b_2	c_2
1	3.4966	3115.61	0.6441	14.79	—	—	—
4	3.4031	2971.02	0.3520	7.873	0.0137	0.2130	−0.2307
9	3.3881	2951.98	0.3447	7.680	0.0131	0.2218	−0.2617
16	3.3833	2946.48	0.3436	7.647	0.0130	0.2257	−0.2675
25	3.3812	2944.28	0.3435	7.640	0.0129	0.2276	−0.2691

Table 4. Values of R on the neutral curves for $a = 2$

Mode	N	q 1.2	2.4	3.6	4.8	6.0
EE1	10	1893.28	1786.57	1794.13	2348.76	3487.55
	16	1869.11	1785.16	1793.28	2348.04	3486.97
	25	1859.61	1783.99	1792.78	2347.51	3486.27
EE2	10	2659.39	1920.56	2115.47	2797.11	4066.66
	16	2435.16	1907.17	2103.75	2788.97	4059.44
	25	2404.30	1902.29	2098.91	2785.30	4056.16
OE1	10	1894.67	1773.19	1901.35	2510.27	3699.13
	16	1877.01	1769.86	1898.11	2507.25	3696.36
	25	1868.43	1768.35	1896.59	2505.70	3694.63
OE2	10	2736.32	2168.03	2448.04	3229.31	4613.61
	16	2343.81	2138.11	2429.10	3213.13	4598.37
	25	2311.75	2126.52	2421.94	3206.86	4592.26

Also, critical values of R and q are located by iterative adjustment of a quadratic interpolation to the neutral curve near its minimum point. Gaussian elimination completes the determination of the coefficients a_k, b_k and c_k, and a normalization $c_1 = 1$ is adopted.

Checks on the influence of the truncation level N were carried out, both in terms of its effect on the position of the neutral curve and in terms of the accuracy of the representation of the original partial differential equations. Results for the square channel (Table 3) show good overall convergence for the leading mode and a comprehensive set of results for a wider channel ($a = 2$, Table 4) indicates diminishing but still adequate convergence both at extreme aspect ratios and for higher modes of convection. Figure 1 gives an indication of accuracy in terms of pointwise satisfaction of the original equations. Here individual terms in equation (5) have been evaluated at $y = z = \frac{1}{4}$ for a square channel with $N = 16$, summed, and plotted as a function of the number of terms retained in the Galerkin series (10). The main variation, which arises from the fourth-order derivative terms, appears to settle down in a satisfactory manner, given the pointwise nature of the comparison. A corresponding analysis of equation (7) indicates relatively little variation and rapid convergence, owing to the reduced order of the derivatives involved.

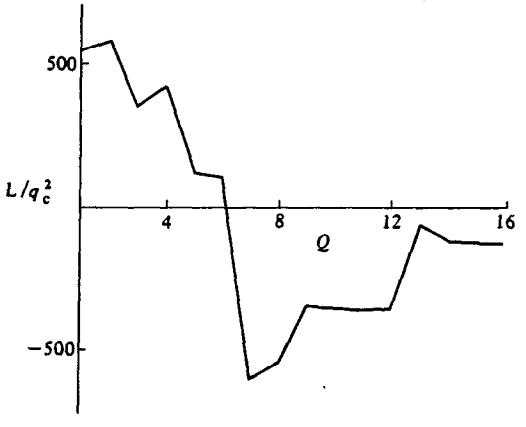

FIG. 1. The behaviour of L/q_c^2, where L is the left-hand side of equation (5), as a function of Q, the number of terms retained in the Galerkin series (10), for $a = \frac{1}{2}$, $N = 16$ and $y = z = \frac{1}{4}$ at the critical point.

3. RESULTS

Figures 2–5 show neutral curves obtained with $N = 25$ for aspect ratios $a = \frac{1}{4}, \frac{1}{2}, 1$ and 2. Except for the lowest aspect ratio, the four leading modes EE1/2, OE1/2 are shown in each case. The qualitative behaviour is similar to that found in ref. [5] for the idealized problem with stress-free horizontal boundaries. The critical Rayleigh number R_c is always that associated with the lowest even mode (EE1) and the corresponding critical wave number increases indefinitely as the aspect ratio decreases. The precise behaviour as $a \to 0$ determined in ref. [6] is

$$R_c \sim \frac{\pi}{16a^4} + \frac{2\sqrt{3}\pi^2}{a^3}, \quad q_c \sim \left(\frac{2\sqrt{3}}{a}\right)^{1/2} \quad (a \to 0). \tag{13}$$

At long wavelengths the lowest odd mode (OE1) can be more dangerous than the corresponding even mode and for low values of a has its minimum at $q = 0$, again consistent with asymptotic predictions

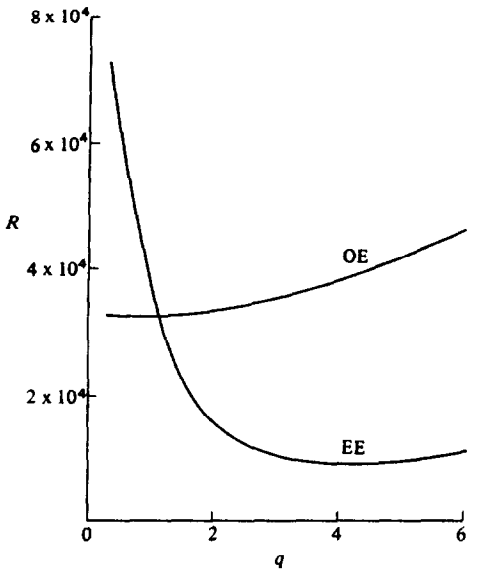

FIG. 2. Neutral curves for the leading even (EE) and odd (OE) modes with $a = \frac{1}{4}$ and $N = 25$.

for $a \to 0$ reported in ref. [6]. At higher aspect ratios the minimum shifts to non-zero values of q, attaining the value $q = 3.117$ associated with an infinite plane layer as $a \to \infty$.

Table 5 shows the critical Rayleigh number R_c and wave number q_c for each of the four aspect ratios

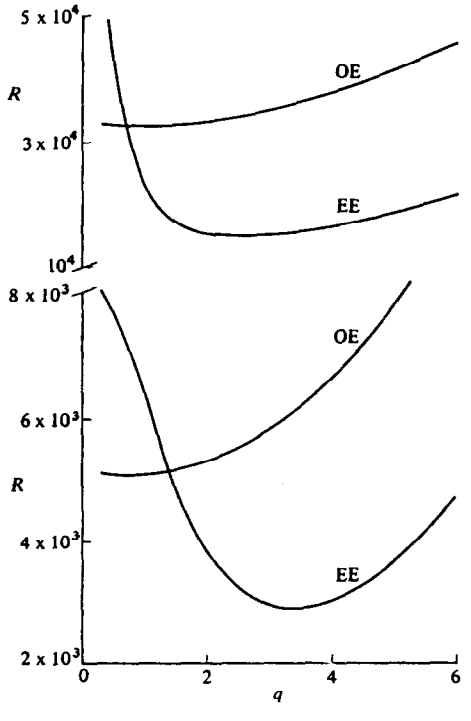

FIG. 3. Neutral curves for the first two even (EE) and odd (OE) modes with $a = \frac{1}{2}$ and $N = 25$.

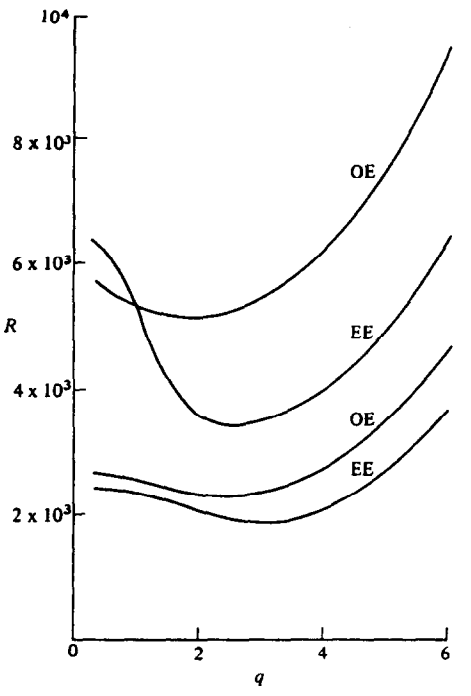

FIG. 4. Neutral curves for the first two even (EE) and odd (OE) modes with $a = 1$ and $N = 25$.

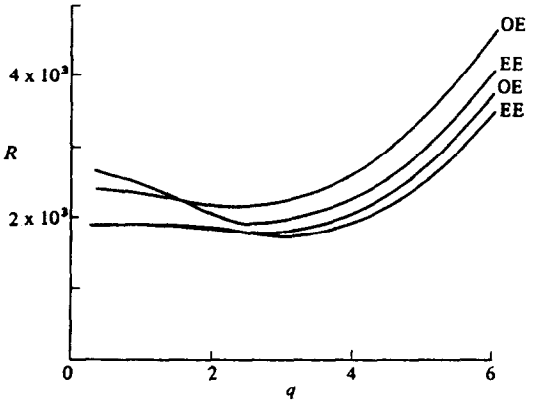

FIG. 5. Neutral curves for the first two even (EE) and odd (OE) modes with $a = 2$ and $N = 25$.

Table 5. Critical wave numbers and Rayleigh numbers for the leading EE modes with $N = 25$

	EE1		EE2	
a	q_c	R_c	q_c	R_c
$\frac{1}{4}$	4.1884	8955.15	—	—
$\frac{1}{2}$	3.3812	2944.28	2.5027	14976.7
1	2.9484	1870.08	2.5318	3424.23
2	2.9983	1719.00	2.5642	1891.85

considered, improving upon the accuracy of the original results for $N = 10$ given in ref. [6]; the minimum point of the neutral curve associated with mode EE2 is also shown.

Table 6. Comparison of asymptotic formulae (14) with numerical results for $a = 2$

Mode	Asymptotic q_c	Asymptotic R_c	Galerkin q_c	Galerkin R_c
EE1	2.9861	1716.48	2.9983	1719.00
OE1	2.5724	1747.29	2.6571	1760.27
EE2	2.2835	1861.36	2.5642	1891.85
OE2	1.3027	2063.56	2.3240	2125.30

The numerical results can also be compared with asymptotic solutions for large aspect ratios. As $a \to \infty$, minima of the neutral curves associated with the leading vertical mode are given by

$$R \sim R_0 + a^{-4}\bar{R}^2/9c, \quad q^2 \sim q_0^2 - a^{-2}\bar{q} \qquad (14)$$

where $R_0 = 1707.76$ and $q_0 = 3.117$ are the critical Rayleigh number and wave number for the infinite layer with rigid horizontal boundaries. Here $\bar{R}$ and $\bar{q}$ are eigenvalues of the reduced system

$$\left(\frac{d^2}{dY^2} + \bar{q}\right)^2 A - \tfrac{1}{9}\bar{R}^2 A = 0;$$

$$A = \frac{dA}{dY} = 0 \quad (Y = \pm 1) \qquad (15)$$

and $c \approx 0.154$ (see ref. [6]). If $\bar{q} < \frac{1}{3}\bar{R}$ even modes (EE) are associated with solutions of

$$\omega_+ \tan \omega_+ + \omega_- \tanh \omega_- = 0 \qquad (16)$$

and odd modes (OE) with solutions of

$$\omega_+ \cot \omega_+ - \omega_- \coth \omega_- = 0 \qquad (17)$$

where $\omega_\pm = (\frac{1}{3}\bar{R} \pm \bar{q})^{1/2}$. If $\bar{q} > \frac{1}{3}\bar{R}$ these equations are replaced by

$$\omega_+ \tan \omega_+ - \omega \tan \omega = 0 \qquad (18)$$

and

$$\omega_+ \cot \omega_+ - \omega \cot \omega = 0 \qquad (19)$$

respectively, where $\omega = (\bar{q} - \frac{1}{3}\bar{R})^{1/2}$. Equations (16)–(19) define the locations of the neutral curves near (q_0, R_0) as $a \to \infty$, with higher modes corresponding to increasing numbers of zeros in the even (EE) or odd (OE) eigenfunction $A(Y)$. The close grouping of the curves is reflected in the results of Fig. 5 for $a = 2$. Minimum values of $\bar{R}$ for the even modes are found to occur where $\frac{1}{3}\bar{R} > \bar{q}$ and equation (16) applies, while minimum values for the odd modes are found to occur where $\frac{1}{3}\bar{R} < \bar{q}$ and equation (19) applies. Numerical solutions of equation (16) or (18) can be initiated from the point where $\bar{q} = \frac{1}{3}\bar{R} = \frac{1}{2}M^2\pi^2$, each integer value of $M(=1, 2, \ldots)$ corresponding to a different solution branch. Minima of the leading even branches are found at

$$(\bar{q}, \bar{R}) = (3.1959, 13.905), (18.005, 58.363), \ldots \qquad (20)$$

while minima of the leading odd branches are found at

$$(\bar{q}, \bar{R}) = (12.394, 29.609), (32.075, 88.826), \ldots \qquad (21)$$

Overall minima for R given by expression (14) when $a = 2$ are consistent with the results of the Galerkin method for this aspect ratio (see Table 6). However, for the higher branches the departure from the asymptotic form is rapid, particularly in terms of the wavelength of the motion.

Acknowledgement—This work was carried out with the support of an SERC research grant.

REFERENCES

1. S. H. Davis, Convection in a box: linear theory, *J. Fluid Mech.* **30**, 465–478 (1967).
2. I. Catton, Convection in a closed rectangular region. The onset of motion, *J. Heat Transfer* **92**, 186–190 (1970).
3. K. Buhler, K. R. Kirchartz and H. Oertel, Steady convection in a horizontal fluid layer, *Acta Mechanica* **31**, 155–161 (1979).
4. J. M. Luijkx, J. K. Platten and J. C. Legros, Precise measurements of the wavelength at the onset of Rayleigh–Bénard convection in a long rectangular duct, *Int. J. Heat Mass Transfer* **25**, 1252–1254 (1982).
5. R. P. Davies-Jones, Thermal convection in an infinite channel with no-slip sidewalls, *J. Fluid Mech.* **44**, 695–704 (1970).
6. M. S. Chana and P. G. Daniels, Onset of Rayleigh–Bénard convection in a rigid channel, *J. Fluid Mech.* **199**, 257–279 (1989).
7. D. L. Harris and W. H. Reid, On orthogonal functions which satisfy four boundary conditions—II, *Astrophys. J. Suppl. Series* **3**, 448–488 (1958).
8. J. M. Luijkx and J. K. Platten, On the onset of free convection in a rectangular channel, *J. Non-equilib. Thermodyn.* **6**, 141–158 (1981).

STABILITE LINEAIRE DE LA CONVECTION DANS UN CANAL RIGIDE CHAUFFE UNIFORMEMENT PAR LE BAS

Résumé—Une formulation bidimensionnelle de Galerkin des équations tridimensionnelles d'Oberbeck–Boussinesq est utilisée pour déterminer l'apparition de la convection dans un canal infini, horizontal, rigide et uniformément chauffé par le bas. Des résultats antérieurs (Chana et Daniels, *J. Fluid Mech.* **199**, 257–259 (1989)) sont étendus à des niveaux plus élevés de troncature et on inclut des modes de convection non examinés jusqu'ici.

LINEARE STABILITÄT DER KONVEKTION IN EINEM VON UNTEN GLEICHMÄSSIG BEHEIZTEN KANAL

Zusammenfassung—Das Ziel ist, den Beginn der Konvektion in einem unbegrenzten, stabilen, waagerechten, von unten gleichmäßig beheizten Kanal zu bestimmen. Dazu wird ein zweidimensionaler Galerkin-Ansatz der dreidimensionalen Oberbeck–Boussinesq-Gleichungen benutzt. Gegenüber früheren Ergebnissen (Chana and Daniels, *J. Fluid Mech.* **199**, 257–279 (1989)) werden die Abbruchbedingung erweitert und bisher nicht untersuchte Arten der Konvektion eingebunden.

ЛИНЕЙНАЯ УСТОЙЧИВОСТЬ КОНВЕКЦИИ В ЖЕСТКОМ КАНАЛЕ, ОДНОРОДНО НАГРЕВАЕМОМ СНИЗУ

Аннотация—Для определения возникновения конвекции в неограниченном жестком горизонтальном канале, однородно нагреваемом снизу, используются трехмерные уравнения Обербека–Буссинеска в двумерной формулировке Галеркина. Ранее полученные результаты (Chana and Daniels, *J. Fluid Mech.* **199**, 257–279 (1989)) распространяются на более высокие уровни замыкания и для учета неисследованных моД конвекции.